Monthly Notices
of the
ROYAL ASTRONOMICAL SOCIETY

MNRAS **446,** 943–958 (2015) doi:10.1093/mnras/stu2093

Optical supernova remnants in nearby galaxies and their influence on star formation rates derived from Hα emission

M. M. Vučetić,[1]★ B. Arbutina[1] and D. Urošević[1,2]

[1]*Department of Astronomy, Faculty of Mathematics, University of Belgrade, Studentski trg 16, 11000 Belgrade, Serbia*
[2]*Isaac Newton Institute of Chile, Yugoslavia Branch*

Accepted 2014 October 7. Received 2014 October 7; in original form 2014 April 15

ABSTRACT

In this paper, we present the most up-to-date list of nearby galaxies with optically detected supernova remnants (SNRs). We discuss the contribution of the H α flux from the SNRs to the total H α flux and its influence on the derived star formation rate (SFR) for 18 galaxies in our sample. We found that the contribution of SNR flux to the total H α flux is 5 ± 5 per cent. Due to the observational selection effects, the SNR contamination of SFRs derived herein represents only a lower limit.

Key words: stars: formation – ISM: supernova remnants – galaxies: ISM – galaxies: star formation.

1 INTRODUCTION

Understanding and modelling star formation rates (SFRs) are the central goals of the theory of star formation. SFR is one of the crucial ingredients of cosmological simulations of galaxy formation, which demonstrate the impact of SFR models on galaxy evolution. SFR has been a major issue in astrophysics since the 1970s, and during the last two decades, the cosmic star formation history of the Universe has been widely studied to constrain galaxy formation and evolution models better.[1] Large-area surveys and larger telescopes have improved our knowledge of SFRs at low to intermediate red shifts ($z < 1.0$) (see Hopkins & Beacom 2006) and beyond (e.g. Karim et al. 2011; Sobral et al. 2013). These studies show a strong decrease of SFR towards the present epoch, and they suggest that star formation over the last ∼11 Gyr is responsible for producing ∼95 per cent of the total stellar mass density observed locally.

Determination of SFRs in galaxies through the Hubble sequence provides vital clues to the evolutionary histories of galaxies. Measured SFRs are spread along six orders of magnitude (when normalized by galaxy mass), from almost zero in gas-poor elliptical, disc and dwarf galaxies, up to ∼100 $M_\odot$ yr^{-1} in optically selected starburst galaxies, or even more in the most luminous infrared (IR) starburst galaxies (Kennicutt 1998).

The first quantitative SFRs were derived from evolutionary synthesis models of galaxy colours (Searle, Sargent & Bagnuolo 1973). Later, more precise diagnostic tools used integrated emission-line fluxes (Kennicutt 1983), near-ultraviolet (UV) continuum fluxes (Donas & Deharveng 1984) and IR continuum fluxes (Rieke & Lebofsky 1978). Nowadays, many different properties are used as star formation tracers, with the goal of directly or indirectly targeting a continuum or line emission that is sensitive to short-lived massive stars. Also, different techniques are used depending on whether we measure SFRs for a whole galaxy or for regions within a galaxy (e.g. molecular clouds). The most common approach for measuring SFRs in resolved regions is to count individual objects, e.g. young stellar objects, or events, e.g. supernovae (SNe), that trace recent star formation. Calibrations of SFR indicators have been made using X-rays, UV light, optical light, IR light and all the way to radio waves, using both continuum and line emission. For a recent review of the latest achievements in the field, see Kennicutt & Evans (2012), as well as the previous review by Kennicutt (1998).

In this paper, we focus on better constraining SFRs from the H α emission line. The next section will introduce star formation measurements made using this emission line.

1.1 Star formation rates from the H α flux

Nebular emission lines are very effective in re-emitting stellar luminosity, and thus allow direct measurement of young stellar content in a galaxy. This is especially the case for the H α line, observationally the strongest of the recombination lines from regions of ionized gas surrounding young hot stars (H II regions). Only stars with masses exceeding 10 $M_\odot$ contribute significantly to the stellar flux, which can ionize the interstellar medium (ISM). Also, these stars have a lifetime shorter than 20 Myr, so the emission lines give us almost instantaneous SFRs, independent of previous star formation histories. The conversion factor between integrated emission-line luminosity and SFR is computed using stellar evolutionary synthesis models. While calibrations have been published by numerous authors, here we use the calibration from Kennicutt, Tamblyn & Congdon (1994), which assumes solar abundances and the Salpeter initial mass function (IMF) (Salpeter 1955) for stellar masses in the range 0.1–100 $M_\odot$:

$$\mathrm{SFR}\ (M_\odot\ \mathrm{yr}^{-1}) = 7.94 \times 10^{-42} L_{\mathrm{H}\alpha}\ (\mathrm{erg\ s}^{-1}), \quad (1)$$

★ E-mail: mandjelic@matf.bg.ac.rs

[1] Some recent models, however, show that galaxies self-regulate – star formation is regulated by stellar feedback (radiation, stellar winds and supernovae) limiting the amount of very dense gas available for forming stars (Hopkins, Quataert & Murray 2011).

which gives the calibration coefficient for the Case B recombination at $T_e = 10\,000$ K. There is a significant variation among published values for this calibration coefficient (∼30 per cent). The differences in coefficient values originate from differences in stellar evolution, atmosphere models and IMFs.

The method for deriving SFRs from the H α flux is one of the most used methods due to the advantages of optical observations and strength of the H α line. Star formation in nearby galaxies can be mapped at high resolution even with small telescopes, and the H α line can be detected in the red-shifted spectra of starburst galaxies up to $z < 3$ (Bechtold et al. 1997; Geach et al. 2008; Sobral et al. 2013).

The main limitations of the method are its sensitivity to uncertainties in extinction and the IMF, and the assumption that the formation of all massive stars is traced by the ionized gas. There is a fraction between 15 and 50 per cent of ionizing radiation that escapes from H II regions. This can be measured either directly (Oey & Kennicutt 1997), or from observations of the diffuse H α emission in nearby galaxies. In their analysis of diffuse H α emission, Ferguson et al. (1996) found that diffuse ionized gas is photoionized by Lyman continuum photons that have escaped from H II regions. Therefore, diffuse H α emission should be included when this SFR measurement method is used.

The dominant source of systematic error in SFR measurements from H α fluxes is extinction within the galaxy observed. Internal extinction can be corrected by combining H α line and IR continuum emission or radio data (Kennicutt et al. 2009), which are not affected by extinction. Mean extinction values range from $A(\mathrm{H}\,\alpha) = 0.5$ to 1.8 mag (see Kennicutt (1998) and James et al. (2005) and references therein), depending on galaxy type and luminosity. As this extinction correction comes with large uncertainty, and therefore represents a large change (two to three times higher) in derived fluxes, it was usually not applied when calculating SFRs. With recent IR surveys (*Spitzer*, *Herschel* and *WISE*), which give estimates for the amount of dust in nearby galaxies, extinction correction is more commonly considered.

Also, we emphasize the importance of eliminating H α flux contaminants when calculating SFRs from H α emission. Emission spectra from H II regions show that very close to the H α line, on both sides, are [N II] lines at λ654.8 and λ658.3 nm. Most of the filters used to extract H α lines also let some of the [N II] emission pass through. This problem can be minimized by using different methods. However, some uncertainty still remains in derived H α fluxes. Using spectroscopic observations, we can calculate the ratio between the H α and [N II] lines, and using filter profiles we can obtain corrections for [N II] contamination. Another possibility is to use very narrow [N II] filters for deriving this correction (James et al. 2005). However, because of the gradient in [N II] abundances with a change of galactocentric distance, one should be careful when applying any correction. The most commonly used corrections for [N II] emission for entire galaxies are those derived by Kennicutt (1983) and Kennicutt & Kent (1983). Using galaxies from Sloan Digital Sky Survey Data Release 4 (Adelman-McCarthy et al. 2006), a simple correction has also been derived by Villar et al. (2008) and presented by Sobral et al. (2012) and is now widely used.

Another origin of H α flux contamination are the sources that emit H α radiation but which are not H II regions surrounding young high-mass OB stars. There is a wide range of such objects that cause an overestimate of SFRs: other emission nebulae, such as planetary nebulae (PNe) and supernova remnants (SNRs); active galactic nuclei (AGNs); ultraluminous X-ray sources (ULXs) and their surrounding nebulae; microquasars; foreground stars with H α emission and superbubbles. None of these types of object have so far been thoroughly discussed as possible sources of systematic error in H α flux-based determination of SFRs.

Some papers have described efforts to exclude emission from PNe when making catalogues of H II regions and estimating SFRs. Azimlu, Marciniak & Barmby (2011) did this for the M31 galaxy. When they removed all PNe candidates, they found that PNe were responsible for 1 per cent of the total measured Hα emission. The problem with PNe, as well as with SNRs, is that they are hard to differentiate from compact H II regions based on H α emission only. Additional observations in narrow-band filters can certainly distinguish between different emission nebulae types. Also, PNe are much smaller in size compared to the majority of H II regions. These can be compact, the same size as PNe (smaller than a parsec), if they are excited only by a single star, but H II regions are generally larger, being excited by multiple young massive stars, or even clusters. On the other hand, SNRs can also vary in size, ranging from compact (a few parsecs) to huge (up to 100 pc) (Čajko, Crawford & Filipović 2009), depending on the phase of their evolution, as well as on the input energy from the SN explosion and surrounding ISM density.

Some AGNs are prominent in the H α line from their broad-line and narrow-line regions (depending on the red shift and the inclination angle). But, considering their small size, and certainly a modest number of them can be detected in the projection of a single galaxy, their contribution to the total H α flux of a galaxy may be negligible. On the other hand, there have been efforts to exclude AGNs from a sample of star-forming galaxies with high red shift, which have been studied for SFRs (Garn et al. 2010; Villar et al. 2011).

ULX sources are compact X-ray sources located away from the nucleus of their host galaxy, emitting well above the Eddington limit of a 20 $M_\odot$ black hole ($L_X \sim 3 \times 10^{39}$ erg s^{-1}). Recently, more and more ULX sources have been detected with strange nebular emissions surrounding them. They include IC342 X-1 in the IC342 galaxy (Roberts et al. 2003; Abolmasov et al. 2007; Feng & Kaaret 2008), Holmberg IX X-1 in the Holmberg IX galaxy (Fabbiano 1988; Gladstone, Roberts & Done 2009; Moon et al. 2011; Grisé et al. 2011) and MF 16 (nomenclature from Matonick & Fesen 1997) in NGC 6946 (Roberts & Colbert 2003). Most likely this nebular emission is from an accretion disc. Such nebulae are also prominent in the H α line and, as such, are potential contaminants of the H α flux and instantaneous SFRs. Of course, ULX sources can be regarded as tracers of some past SFRs. For the NGC 6946 galaxy, the flux of MF 16 is responsible for 0.1 per cent of the total H α flux, as is the case with the IC342 galaxy and IC342 X-1 source. On the other hand, as Andjelić (2011) has shown, H α derived SFRs for the Holmberg IX galaxy can be significantly changed if nebular emission from the ULX is removed from the integrated H α flux of the galaxy. Emission from HoIX X-1 is responsible for 75 per cent of the H α emission from this dwarf galaxy. We adopt the H α flux of this object from Arbutina et al. (2009).

Microquasars are X-ray binary systems with an accretion disc, relativistic jets and, usually, strong and variable radio emission. Also, they can have a surrounding emission nebula. The large nebula S26 (from Blair & Long 1997) in the nearby galaxy NGC 7793 is a jet-inflated bubble around a powerful microquasar (Pakull, Soria & Motch 2010). The H α emission from this source is not a tracer of star formation, and it is responsible for 1.15 per cent of the galaxy's total H α emission.

Foreground emission-line stars, such as O and B supergiants and Wolf–Rayet stars, have strong optical emission lines, primarily hydrogen Balmer lines. In most of these systems, the emission

originates from strong stellar winds. While these stars have strong emission, they also have a very bright continuum, and therefore they should be easily distinguished from H II regions. Hence, foreground emission-line stars could easily be removed from the total H α flux and should not represent a source of error in H α derived SFRs.

Superbubbles are regions of bright emission that frequently surround an OB association. This kind of nebula is powered by a combination of stellar winds, UV stellar radiation and occasional SN explosions. On the other hand, wind-blown nebulae are related to the H II regions, but they are ionized due to shock fronts caused by strong stellar winds. Superbubbles are characterized by low-velocity shock fronts (<100 km s^{-1}), while classical SNRs have shock fronts expanding at 100–1000 km s^{-1}. With modern observational equipment, superbubbles can be distinguished from SNRs, mostly on detecting OB associations inside them. In the M31 SNR survey, Lee & Lee (2014) separated 44 superbubbles from previous SNR candidates, which represent 1.3 per cent of the total H α emission of this galaxy. For the M101 galaxy, 10 superbubbles represent 0.3 per cent (Franchetti et al. 2012).

The main aim of this paper is to estimate the influence of SNR emission on the H α derived SFRs. To do so, we assemble a current sample of optically detected SNRs in nearby galaxies.

In the next section we discuss the optical detection of SNRs. Section 3 gives details of the individual galaxies in our sample and the detection of SNRs in those galaxies, while in Section 4 we discuss the influence of SNR emission on the H α derived SFRs. In Section 5 we present our conclusions.

2 OPTICAL DETECTION OF SNRS

Optical extragalactic searches for SNRs were pioneered by Mathewson & Clarke (1973a). They used the fact that the optical spectra of SNRs have elevated [S II] λ671.7 and λ673.1 nm to H α λ656.3 nm emission-line ratios, compared to the spectra of normal H II regions. These emission ratios have been used to differentiate between shock-heated SNRs (ratios >0.4, but often considerably higher) and photoionized nebulae (<0.4, but typically <0.2) (Blair & Long 2004). This is justified by their different ways of excitation. For SNRs, collisional excitation is induced by shocks, rather than by photoionization, which is the case with H II regions. In typical H II regions, sulfur exists mainly in the form of S^{++}, yielding low [S II] to H α emission ratios. For SNRs, after the shock wave from an SNR propagates through the surrounding medium and as the material cools sufficiently (when an SNR is in the radiative phase), a variety of ionization states are present, including S^{+}. This is the phase when the SNRs are most prominent in optical wavelengths and when we expect the increased [S II]/H α ratios to be observed in SNRs.

The classical definition for detection of an SNR at optical wavelengths is [S II]/H α > 0.4. Since the [N II] lines mentioned above may be as strong as ∼50 per cent of the H α line, some authors have relaxed the above criterion for identification of an SNR to the condition [S II]/H α > 0.3. (Dopita et al. 2010a; Leonidaki, Boumis & Zezas 2013).

2.1 Optical observations of SNRs

The optical search for SNRs is usually performed using the narrow-band H α and [S II] filters. Another filter is used to remove the contribution from the continuum radiation. Modern instruments, both telescopes and CCDs, have much improved possibilities for this kind of observation in the recent 15–20 yr. That is why we have seen a significant increase in the number of optically detected SNRs in this period. In recent years, a significant step has been made in producing more complete SNR samples for some galaxies, such as M31, M33 and M83. Earlier, most optical detections of SNRs were performed using photographic plates, which have much lower sensitivity and are more difficult to process. The largest contributions to the number of optically detected SNRs in this early period can be attributed to D'Odorico, Dopita & Benvenuti (1980) and Mathewson et al. (1983, 1984, 1985). Mathewson and his group made a major contribution to the detection in Magellanic Clouds (MCs), while D'Odorico et al. (1980) observed eight galaxies: NGC 6822, IC1613, M31, M33, NGC 253, NGC 300, NGC 2403 and IC342. Both of these groups only detected SNRs, without making any flux measurements.

The next major contribution to this field was also by two groups of authors, Blair & Long (1997) and Matonick & Fesen (1997). The first group observed two galaxies in the Sculptor group, NGC 300 and NGC 7793, while Matonick & Fesen (1997) observed five nearby spiral galaxies, NGC 5204, NGC 5585, NGC 6946, M81 and M101. Also, in the same year Matonick et al. (1997) published observations of spiral galaxy NGC 2403.

Matonick & Fesen (1997) used the 1.3-m McGraw-Hill Telescope at the Michigan-Dartmouth-MIT Observatory. They took sets of three images through each filter, with exposure times ranging from 300 to 1200 s. They also made spectroscopic observations, which they used both to confirm detections and to calibrate the H α flux for the [N II] contamination.

Blair & Long (1997) made observations using the 2.5-m du Pont Telescope at Las Campanas Observatory. They managed 1500-s exposure times with the H α filter (but it should be noted that their filters had a slightly lower transmittance of 50–60 per cent), while exposure times were at least twice as long for the [S II] filter as for H α, to permit comparable signal-to-noise ratios in objects having [S II]/H α ratios of ∼0.5. They applied a flat correction of 25 per cent to remove [N II] contamination from the H α images.

Recently, Leonidaki et al. (2013) made a major contribution to the total number of optically detected SNRs in nearby galaxies. For six galaxies (NGC 2403, NGC 3077, NGC 4214, NGC 4395, NGC 4449 and NGC 5204), they detected more than 400 SNRs. They carried out a multiwavelength analysis of SNRs in these six galaxies, using both their optical observations and the X-ray observations published previously by Leonidaki, Zezas & Boumis (2010). Leonidaki et al. (2013) obtained optical images with the 1.3-m Ritchey-Chrétien Telescope at the Skinakas Observatory. They used a 3600-s exposure time with the H α filter and 7200-s with the [S II] filter. To estimate the H α flux of their objects, they made a correction for [N II] contamination using the [N II](λλ6548, 6584)/H α ratios from the integrated spectroscopy of the galaxies in the work of Kennicutt et al. (2008).

Also, over the last 10 yrs, several studies have used very large telescopes for SNR surveys. This has resulted in several excellent SNR samples for nearby galaxies, such as M31, M33 and M83. Lee & Lee (2014) used data provided by the Local Group Survey (Massey et al. 2006) obtained with the 4-m Mayall Telescope at Kitt Peak National Observatory. To detect SNRs in M33, Long et al. (2010) used the same telescope, complemented with very deep exposures using the 0.9-m Burrell Schmidt Telescope. The M83 galaxy was observed using the same 4-m telescope by Blair & Long (2004), but also with the *Hubble Space Telescope* (*HST*) (Dopita et al. 2010a; Blair et al. 2014) and the 6.5-m Magellan Telescope (Blair, Winkler & Long 2012). M83 is the galaxy with the best sample of optically selected SNRs.

Table 1. Data for galaxies which have been observed for optical SNRs.

Galaxy name	R.A. (J2000) (h:m:s)	Decl. (J2000) (d:m:s)	Distance (Mpc)	Distance reference	Major axis (arcmin)	Minor axis (arcmin)	Galactic latitude (°)	Incl.[a] (°)	Galaxy	B (mag)	A_B (mag)
LMC	05:23:34.5	−69:45:22	0.05	1	645	550	−32.9	35	SB(s)m	0.9	0.272
SMC	00:52:44.8	−72:49:43	0.06	2	320	185	−44.3	58	SB(s)m pec	2.7	0.134
NGC 6822	19:44:57.7	−14:48:12	0.50	1	15.5	13.5	−18.4	33	IB(s)m	9.31	0.855
NGC 185	00:38:58.0	48:20:15	0.62	3	11.7	10.0	−14.5	–	E3 pec	10.1	0.667
IC1613	01:04:47.8	02:07:04	0.65	4	16.2	14.5	−60.6	29	IB(s)m	9.88	0.090
IC342	03:46:48.5	68:05:47	3.30	5	21.4	20.9	10.6	25	SAB(rs)cd	9.1	2.024
NGC 253	00:47:33.1	−25:17:18	3.94	6	27.5	6.8	−87.9	85	SAB(s)c	8.04	0.068
M31	00:42:44.3	41:16:09	0.79	4	190	60	−21.6	78	SA(s)b	4.36	0.225
M33	01:33:50.9	30:39:37	0.84	4	70.8	41.7	−31.3	54	SA(s)cd	6.27	0.15
NGC 300	00:54:53.5	−37:41:04	2.0	4	21.9	15.5	−79.4	45	SA(s)d	8.95	0.046
NGC 4214	12:15:39.2	36:19:37	2.92	7	8.5	6.6	78.1	39	IAB(s)m	10.24	0.079
NGC 2403	07:36:51.4	65:36:09	3.22	4	21.9	12.3	29.2	57	SAB(s)cd	8.93	0.145
M82	09:55:52.7	69:40:46	3.53	8	11.2	4.3	40.6	69	I0 edge-on	9.3	0.567
M81	09:55:33.2	69:03:55	3.63	4	26.9	14.1	40.9	62	SA(s)ab	7.89	0.291
NGC 3077	10:03:19.1	68:44:02	3.82	9	5.4	4.5	41.6	38	I0 pec	10.61	0.243
NGC 7793	23:57:49.8	−32:35:28	3.91	6	9.3	6.3	−77.2	48	SA(s)d	9.98	0.053
NGC 4449	12:28:11.1	44:05:37	4.21	9	6.2	4.4	72.4	45	IBm	9.99	0.053
M83	13:37:00.9	−29:51:56	4.47	10	12.9	11.5	31.9	28	SAB(s)c	8.2	0.241
NGC 4395	12:25:48.8	33:32:49	4.61	9	13.2	11.0	81.5	34	SA(s)m?	10.64	0.063
NGC 5204	13:29:36.5	58:25:07	4.65	9	5.0	3.0	58.0	54	SA(s)m	11.73	0.045
NGC 5585	14:19:48.2	56:43:45	5.7	11	5.8	3.7	56.6	51	SAB(s)d	11.2	0.057
NGC 6946	20:34:52.3	60:09:14	5.9	12	11.5	9.8	11.7	32	SAB(rs)cd	9.61	1.241
M101	14:03:12.5	54:20:56	6.7	4	28.8	26.9	59.8	22	SAB(rs)cd	8.31	0.031
M74	01:36:41.7	15:47:01	7.3	13	10.5	9.5	−45.7	20	SA(s)c	9.95	0.254
NGC 2903	09:32:10.1	21:30:03	8.9	14	12.6	6.0	44.5	64	SAB(rs)bc	9.68	0.113

[a]From Tully (1988).

DISTANCE REFERENCES: (1) van den Bergh (2000); (2) Ferrerese et al. (2000); (3) Conn et al. (2012); (4) Freedman et al. (2001); (5) Saha, Claver & Hoessel (2002); (6) Karachentsev et al. (2003a); (7) Tully et al. (2006); (8) Sakai & Madore (1999); (9) Karachentsev et al. (2003b); (10) Thim et al. (2003); (11) Karachentsev, Kopylov & Kopylova (1994); (12) Karachentsev et al. (2004); (13) Sharina, Karachentsev & Tikhonov (1996); (14) Drozdovsky & Karachentsev (2000).

2.2 Galaxies with optically identified SNRs

To estimate the contribution from SNRs to the total H α emission used to determine SFRs in a galaxy, we searched the literature for all galaxies that have optically identified SNRs. In total, there are 25 of them (excluding the Milky Way). They are listed in Table 1, with basic data for each galaxy taken from the NASA Extragalactic Database (NED).[2]

Note that in Table 1 there are galaxies, such as NGC 253 and IC342, that do not have published flux estimates for their SNRs. For the NGC 185 galaxy, we did not find any published H α flux. Also, there are galaxies (such as the Large Magellanic Cloud (LMC), Small Magellanic Cloud (SMC), NGC 6822 and IC1613) that have not been surveyed for optical SNRs, but detection of individual SNRs has been presented in the literature. None of these seven galaxies listed in the first part of Table 1 will be included in our discussion on SNR contribution to the H α derived SFRs. We wll give a few details of the optical detection of SNRs in each of these galaxies, as a guide for future work in this field.

The LMC and the SMC are the closest neighbours of the Milky Way. Due to their proximity, studies of SNRs in these galaxies began as early as the 1960s. At the distance of the MCs (50–60 kpc), SNRs are well resolved, which gives an opportunity for more in-depth analysis. This is why an increasing number of recent papers on SNRs in the MCs discuss individual objects (e.g. Bozzetto et al. 2012a,b) but through multifrequency analysis (e.g. Bozzetto et al. 2012c; de Horta et al. 2012; Haberl et al. 2012a; Maggi et al. 2012; Bozzetto et al. 2013; Bozzetto et al. 2014).

The first detection of SNRs in the MCs was made using a combination of radio and optical techniques (Mathewson & Clarke 1972, 1973a, 1973b; Mathewson et al. 1983, 1984, 1985).

Filipović et al. (1998) listed all the discrete radio sources in the Parkes survey of the MCs, and found 32 SNRs and 12 SNR candidates in the LMC, and 12 SNRs in the SMC. Filipović et al. (2005) presented 16 radio SNRs in the SMC found with the Australian Telescope Compact Array (ATCA). 12 of them have optical long-slit spectra and estimated line ratios, as presented by Payne et al. (2007). According to Payne, White & Filipović (2008), a revision of the Parkes survey complemented with ATCA data yielded 52 confirmed SNRs and 20 candidates in the LMC.

Williams et al. (1999) published an atlas of *ROSAT* X-ray sources, which contained 31 LMC SNRs, while Haberl et al. (2012b) were the first to cover the full extent of the SMC at X-ray wavelengths.

Badenes, Maoz & Draine (2010) discussed the size distribution of SNRs in the MCs. They tried to collect a full sample of SNRs in the MCs. They merged two online catalogues to obtain 54 confirmed SNRs in the LMC and 23 in the SMC. The first catalogue is an optical catalogue of MC SNRs being assembled as part of the Magellanic Clouds Emission Line Survey (Smith, Leiton & Pizarro 2000); the most recent on-line version of this catalogue[3] lists 31 SNRs in

[2] http://ned.ipac.caltech.edu/

[3] http://www.ctio.noao.edu/mcels/snrs/framesnrs.html

the LMC and 11 in the SMC. The second catalogue is the Magellanic Clouds Supernova Remnant Database (Murphy Williams et al. 2010);[4] the current version of this catalogue contains 47 confirmed objects in the LMC and 16 in the SMC. Unfortunately, neither of these catalogues contains data on optical fluxes.

NGC 6822 is one of the nearest dwarf irregular galaxies in the Local Group. Despite its convenient distance, only one SNR has been detected so far. This SNR, Ho12, was first observed by Hodge (1977), and later by D'Odorico et al. (1980) and D'Odorico & Dopita (1983). Kong, Sjouwerman & Williams (2004) published a multiwavelength analysis of this SNR.

NGC 185 is a dwarf elliptical companion of the Andromeda Galaxy, which has undergone recent star formation activity. Gallagher, Hunter & Mould (1984) obtained spectra for NGC 185, and found a strong [S II] emission, which originated from an SNR. Later, Martínez-Delgado, Aparicio & Gallart (1999) obtained new H α observations of the central region of NGC 185, and they also detected this SNR. Finally, Gonçalves et al. (2012) confirmed this object is a SNR using deep spectroscopy.

IC1613 is a low-mass irregular galaxy in the Local Group. The only known SNR in this galaxy is the bright nebula S8 (Sandage 1971). This SNR has been observed by numerous authors (D'Odorico et al. 1980; D'Odorico & Dopita 1983; Peimbert, Bohigas & Torres-Peimbert 1988) and a complete multiwavelength analysis was presented by Lozinskaya et al. (1998).

IC342 is an almost face-on spiral galaxy of large angular extent. It is heavily obscured by the Galactic disc, and this is why it has often been avoided for optical observations. D'Odorico et al. (1980) were the first to search for IC342 SNRs at optical wavelengths. They detected four SNRs, but observed only the central part of the galaxy. Vučetić et al. (2013) searched for SNRs and H II regions in the south-western part of this galaxy using H α and [S II] filters. Until now, Vučetić et al. (2013) have published only detections of H II regions, while results for SNRs are in preparation.

NGC 253 is one of the nearest starburst galaxies. Detecting SNRs in this galaxy is difficult because of ita edge-on orientation. Most SNR surveys of this galaxy have been in the radio domain (Ulvestad 2000; Lenc & Tingay 2006). Optically, so far only two SNR candidates have been detected, both by D'Odorico et al. (1980).

2.3 Sample selection

From the 25 galaxies that have optical SNRs, we selected 18 that have been fully or partially surveyed for SNRs in optical wavelengths and which have published flux estimates for SNRs. These galaxies are listed in the second part of Table 1.

When we look at the morphologies of the galaxies in the sample, 14 of them are spirals and four are irregular galaxies. Since spiral and irregular galaxies are where most star births occur, it is hardly surprising that such galaxies have been chosen as targets for optical searches for SNRs. Most of the galaxies have lower inclinations to reduce internal extinction, with the exception of a few bright and well-known galaxies, such as M31 and M82. For the same reason, almost all the galaxies (except NGC 6946) are not in the Galactic plane, having Galactic latitudes $|b| > 20^\circ$, to reduce Galactic extinction. Also, all of the galaxies in our sample have blue apparent magnitude $B < 12$. Half of the galaxies in our sample lie at a distance of 3–5 Mpc. The most distant galaxy with optically detected SNRs is NGC 2903, at a distance of nearly 9 Mpc.

[4] http://www.mcsnr.org/

We queried the Nearby Galaxies Catalog (Tully 1988) to see how many galaxies meet the criteria of our sample: a spiral or irregular galaxy, $d < 9$ Mpc, $i < 70^\circ$, $|b| > 20^\circ$ and $B < 12$. In total, 50 galaxies meet these criteria, while 17 are within 3–5 Mpc. Hence, our sample represents roughly 35 per cent of the galaxies that could be observed for SNRs. The criteria for our sample are simply a consequence of bias – observers tend to choose target objects that are closer, brighter and with less extinction. If we extended conditions to cover all inclinations and to a blue apparent magnitude of $B = 15$, 154 galaxies would be available.

In the sample there are galaxies (like NGC 2403, M83 and M101) with multiple detections of the same SNR by different studies. In such cases, we have taken flux data from the most reliable observations. Also, in cases (such are M83 and M101) where there are observations of different parts of the same galaxy, we naturally present SNRs detected in all of the observed parts.

To compare fluxes of SNRs with H α fluxes of galaxies, we correct the fluxes of SNRs for Galactic extinction and [N II] contamination in the same manner as for fluxes of galaxies (more details are given in Section 4). Such corrected H α fluxes are presented in Section 4, while in the next section we give SNR fluxes for each galaxy as originally published.

3 NEARBY GALAXIES WITH OPTICAL SNRS

In this section, we review the individual galaxies in the sample and their properties. For each galaxy we summarize the history of SNR detection, especially in the optical range, and we specify the characteristics of some unusual sources. We have also collected the H α fluxes of all optically detected SNRs from each galaxy in the sample (which are, together with coordinates, diameters and [S II]/H α ratios, given in the appendix).

3.1 M31

M31, the Andromeda Galaxy, is the largest galaxy in the Local Group and the nearest spiral galaxy to the Milky Way. In many properties, this galaxy is very similar to our own, and that is one of the reasons why it is so interesting to us. It should be mentioned that this galaxy has a small inclination to the line of sight ($\sim 13^\circ$), which is a limiting factor on the number of detectable SNRs. The first discussion of optical SNRs in M31 was by Kumar (1976). DDO80 detected 19 optical SNRs, while Blair, Kirshner & Chevalier (1981) reported 18, with 11 of them having measured line fluxes. Braun & Walterbos (1993) observed a large fraction of the spiral arms in the north-east half of M31 and they detected 52 SNR candidates, at both optical and radio wavelengths. Two years later, Magnier et al. (1995) published a list of 178 SNR candidates, from about one square degree in the galactic disc, but they did not measure the objects' fluxes. At radio wavelengths, Dickel et al. (1982) and Dickel & D'Odorico (1984) searched for radio counterparts to the optical identifications, and they were successful for eight detections. Kong et al. (2003) and Williams et al. (2004) both detected two SNRs, through all three ranges of interest (radio, optical and X-rays), but with roughly calibrated optical data. Using X-rays, Supper et al. (2001) detected 16 SNRs using *ROSAT*, while 21 were identified with *XMM-Newton* (Pietsch, Freyberg & Haberl 2005). Recently, Stiele et al. (2011) published a catalogue of *XMM-Newton* sources from the whole of M31, out of which 25 sources were identified as already known SNRs, while an additional 31 were classified as SNR candidates. Sasaki et al. (2012) searched the Local Group

Galaxy Survey (LGGS)[5] (Massey et al. 2006) and *HST* archival images for optical counterparts to the SNRs and SNR candidates from Stiele et al. (2011). They found that 21 X-ray SNRs have an optical counterpart, as well as 20 X-ray SNR candidates. Also, they suggested an additional five X-ray sources from Stiele et al. (2011) were SNRs, based on their optical properties.

Recently, Lee & Lee (2014) presented a survey of optically emitting SNRs for the entire disc of M31 based on H α and [S II] images from the Local Group Survey. They published a catalogue of 156 SNR candidates in M31. In their survey, they rejected all objects with [S II]/H$\alpha > 0.4$, which also have a number of OB stars in their projection or have sizes $D > 100$ pc. These objects could be H II regions or superbubbles. This is how they decided 154 previously known SNRs were non-SNR objects. Of these 154 non-SNRs, 44 were catalogued as superbubbles. Of 156 SNRs in the catalogue, 80 objects previously detected by Braun & Walterbos (1993), Magnier et al. (1995) and Sasaki et al. (2012), were confirmed to be SNRs.

The total H α flux of 156 SNRs detected in M31 by Lee & Lee (2014) is 4.81×10^{-12} erg cm^{-2} s^{-1}.

3.2 M33

M33 is the nearest late-type spiral galaxy in the Local Group. Its distance of 840 kpc, moderate inclination ($i = 54^{\circ}$) and a low Galactic absorption ($A_B = 0.15$ mag, NED) make this galaxy a good target for an SNR search. This could be the reason why M33 is surely the galaxy with the largest sample of SNRs detected both optically and with X-rays. Long et al. (2010) made an enormous contribution to this topic by reporting and giving detailed descriptions of 137 SNRs using X-ray, optical and radio wavelengths. They improved the sample of optical SNRs previously made by Gordon et al. (1998), which consisted of 98 SNRs detected with the Kitt Peak 4-m telescope. Long et al. (2010) primarily presented results of the ChASeM33 survey (*Chandra* survey, Plucinsky et al. 2008), but they also made a valuable supporting multiwavelength analysis. They used LGGS (Massey et al. 2006) as well as their own optical observations made with the 0.6-m Burrell Schmidt Telescope, but with very long exposures (5100 s). They produced a sample of 137 SNRs, all visible in the optical range, out of which 131 SNRs were detected also with X-rays. They made new radio observations with the Very Large Array (VLA), but in the high-resolution mode to complement previous VLA observations made by Gordon et al. (1999). Gordon et al. (1999) detected 53 SNRs, all of which were previously suggested as SNRs based on optical imagery. Long et al. (2010) were successful in detecting small-diameter, young remnants and pulsar-wind nebulae candidates and in some cases they resolved the confusion of H II regions with SNRs.

Based on these optical observations, we found that the total H α flux from 137 SNRs detected in M33 is 5.8×10^{-12} erg cm^{-2} s^{-1}.

3.3 NGC 300

NGC 300 is a spiral galaxy, a member of the Sculptor Group of galaxies. NGC 300 is very prominent optically and for H α due to many large H II regions, which are evidence of ongoing star formation (see Butler, Martínez-Delgado & Brandner 2004). The first optical detection of SNR candidates was made by D'Odorico et al. (1980). Later studies (Blair & Long 1997; Pannuti et al. 2000; Payne et al. 2004; Millar et al. 2011) were all, with the exception of Blair & Long (1997), multiwavelength analyses. Blair & Long (1997) performed optical narrow-band imaging and spectroscopy and they proposed 28 SNR candidates. Pannuti et al. (2000) presented their VLA observations, in combination with their own optical observations, archival *ROSAT* X-ray data and optical data from Blair & Long (1997). They reported 17 radio SNR candidates, of which three were known from optical observations. Payne et al. (2004) gave detailed cross-matching of objects previously detected in NGC 300 and detections that they made using ATCA and *XMM-Newton* observations. Finally, Millar et al. (2011) performed spectroscopy for 51 sources from Blair & Long (1997) and Payne et al. (2004), as well as analysing archival images from the *Chandra* X-ray observatory. Based on their spectroscopic analysis, Millar et al. (2011) confirmed 22 out of 28 SNR candidates from Blair & Long (1997). In addition, three of them are also visible at radio wavelengths, and two were detected also in the X-ray domain.

The total integrated H α line flux density from these 22 confirmed SNRs from Millar et al. (2011) is 2.3×10^{-13} erg cm^{-2} s^{-1}.

3.4 NGC 4214

NGC 4214 is a nearby irregular dwarf galaxy currently experiencing a high level of massive star formation. Combining optical, near-IR and UV data, Huchra et al. (1983) concluded that it went through a burst of star formation a few times 10^7 yr ago. This galaxy is one of the several galaxies in which surveys for SNRs have been carried out at X-ray, radio and optical wavelengths. Initially, Vukotić et al. (2005) classified one radio source as an SNR from VLA archival observations of NGC 4214. Afterwards, Chomiuk & Wilcots (2009) found six more radio SNR candidates, and three more objects denoted as SNR/H II, also from the VLA observations. Then Leonidaki et al. (2010) searched for X-ray SNR candidates through archival *Chandra* images, and suggested 11 sources as SNRs or SNR candidates. The same year, Dopita et al. (2010b) detected all the radio SNRs from Chomiuk & Wilcots (2009) using the *HST*. Finally, Leonidaki et al. (2013) detected 92 optical SNRs or SNR candidates, using the [S II]/H α ratio criterion.

These 92 optical SNR candidates in NGC 4214 have a total H α flux of 1.73×10^{-12} erg cm^{-2} s^{-1}.

3.5 NGC 2403

NGC 2403 is a spiral galaxy at a distance of 3.22 Mpc and with an inclination angle of around 60°. This galaxy is the second brightest galaxy in the M81 Group (Karachentsev et al. 2002). It was one of the targets of surveys by Leonidaki et al. (2010, 2013) for X-ray and optical SNRs. Also, it was a target of the DDO80 search, which detected two SNRs. Matonick et al. (1997) made a relatively deep optical search for SNRs in this galaxy. They detected 33 new SNRs, and confirmed two detections of DDO80. VLA observations (Turner & Ho 1994; Eck, Cowan & Branch 2002) found only three radio SNR candidates. Pannuti, Schlegel & Lacey (2007) searched for positional coincidences between their sample of X-ray sources in NGC 2403 and 35 SNRs of Matonick et al. (1997) and known radio SNRs in the galaxy. They found only two matches, one an optical SNR and the other a radio SNR candidate. In addition, Leonidaki et al. (2010) found 15 X-ray selected SNRs, while Leonidaki et al. (2013) detected 149 optical SNRs or SNR candidates. All optical SNRs from Matonick et al. (1997), except SNR-1, which was out of the field of view, were detected by Leonidaki et al. (2013).

[5] Data from LGGS are available at http://www.lowell.edu/users/massey/lgsurvey/.

The total H α line flux density of 150 SNRs detected by Leonidaki et al. (2013) and Matonick et al. (1997) for NGC 2403 is 5.65×10^{-12} erg cm^{-2} s^{-1}. This galaxy is the third by the number of optically detected SNRs, after M83 and M31, but it is the first by the percentage of the H α flux from the SNRs in comparison to the total H α flux from the galaxy.

3.6 M82

M82 is a member of the M81 Galaxy Group, at a distance of 3.53 Mpc. It is one of the nearest and certainly the best-studied starburst galaxy. The active starburst has continued for almost 20 Myr at a rate of about 10 $M_{\odot}$ yr^{-1}. The evidence for such strong star formation includes two (radio) SNe in the last 10 yr. Recently, type Ia SN2014J was detected in this galaxy (Fossey et al. 2014). The active starburst region is in the centre of the galaxy. This region has mostly been avoided for optical observations. Attenuation of light by dust has restricted optical detection of the large population of compact SNRs in the core of M82, which have been studied at radio wavelengths (Kronberg & Wilkinson 1975; Kronberg, Biermann & Schwab 1985; Huang et al. 1994; Muxlow et al. 1994; Fenech et al. 2008, 2010). Therefore, no SNRs were detected at visible wavelengths in M82 until de Grijs et al. (2000) analysed *HST* H α narrow-band images. In a part of the galaxy called M82B, which is considered to be a fossil starburst region, 10 SNR candidates were detected. Interestingly, the optical SNR detection by de Grijs et al. (2000) was not based on the [S II]/H α ratio, but on the conditions that the H α luminosity of SNR should be less than 14×10^{35} erg s^{-1} and that the diameter of an SNR should be less than 100 pc.

The total H α line flux density of the 10 SNRs detected by de Grijs et al. (2000) is 2.20×10^{-15} erg cm^{-2} s^{-1}.

3.7 M81

M81 is a nearby spiral galaxy, the brightest galaxy in its group. M81 forms a very conspicuous physical pair with its neighbour, M82, with whom it had a close encounter a few tens of millions of years ago. The galaxy also contains a low luminosity AGN (Markoff et al. 2008). The only thorough search for SNRs in M81 was made by Matonick & Fesen (1997). In five fields of view, covering the whole disc of this galaxy, and by using the [S II]/H α ratio technique, they detected 41 optical SNRs. 10 yr earlier, in a search for giant H II regions in M81 using the VLA at 6 cm and 20 cm, Kaufman et al. (1987) proposed that five sources could be SNRs, according to their spectral indices. The latest paper on SNRs for the M81 galaxy was by Pannuti et al. (2007). They searched for X-ray counterparts to optical and candidate radio SNRs using observations made with the *Chandra* X-Ray Observatory. Their field of view covered only 23 optical and three radio candidate SNRs, but they found no *Chandra*-detected counterparts.

The total H α line flux density of 41 optical SNRs detected by Matonick & Fesen (1997) is 1.8×10^{-13} erg cm^{-2} s^{-1}.

3.8 NGC 3077

NGC 3077 is a nearby dwarf galaxy, a member of the M81 Galaxy Group. The tidal interaction between galaxies in this group leads to enhanced star formation (Walter et al. 2002). Initially, only three X-ray SNR candidates were detected using *Chandra* observations (Ott, Martin & Walter 2003). Rosa-Gonzalez (2005) found that one of these sources coincides with one of the radio sources they had reported. Later, Leonidaki et al. (2010) detected five SNR candidates, using archival *Chandra* images, and among their five detections two were already known (from Ott et al. 2003) and three were new. Finally, Leonidaki et al. (2013) detected 24 optical SNRs in NGC 3077, of which one had both optical and X-ray counterparts.

Here we also mention Garland, a tidal arm east of the galactic centre. VLA H I observations (Walter et al. 2002) show that this is where 90 per cent of the atomic hydrogen around NGC 3077 is located. Also, Karachentsev & Kaisin (2007) reported that Garland has the highest SFR by luminosity among 150 galaxies of the Local volume with known SFRs. For these reasons, Andjelić et al. (2011) searched for optical SNRs in Garland, but they found no candidates.

The total H α line flux density of 24 optical SNRs detected by Leonidaki et al. (2013) in NGC 3077 is 2.47×10^{-13} erg cm^{-2} s^{-1}.

3.9 NGC 7793

NGC 7793 is a member of the nearby Sculptor Group, at a distance of 3.91 Mpc and an inclination angle of $\sim 50^{\circ}$ (Tully 1988). Its spiral pattern is nearly lost in a general confusion of H II and star formation regions. The SNR population of NGC 7793 has been well studied through optical, radio and X surveys (Blair & Long 1997; Pannuti et al. 2002, 2011). According to these searches, there are 32 SNRs (or SNR candidates) in total. First, Blair & Long (1997) detected 28 SNRs with an optical search with narrow-band H α and [S II] filters. Afterwards, Pannuti et al. (2002) detected five new radio SNR candidates, and two SNRs from Blair & Long (1997) using their own VLA observations. They also examined archival *ROSAT* satellite data and found no additional SNR candidates, but it should be kept in mind that the search for SNRs in this range is complicated by the considerable diffuse X-ray emission throughout the entire disc of this galaxy. Finally, Pannuti et al. (2011) improved X-ray data for NGC 7793 using the *Chandra* observatory, but they only found one SNR previously detected at radio wavelengths, and one SNR, S11 (from Blair & Long 1997), detected both at optical and radio wavelengths. Another interesting object in this galaxy is SNR candidate S26 from Blair & Long (1997). This is a microquasar with a surrounding nebula and has been studied by several authors (Pakull et al. 2010; Soria et al. 2010; Dopita et al. 2012). It is an extended region with a diameter of approximately 260 pc, and with a high [S II]/H α ratio, prominent in the H α line, but it is not a tracer of star formation.

Blair & Long (1997) showed that NGC 7793 does not have a very obvious 'gap' between [S II]/H α ratios for H II regions and SNRs, which could lead to numerous contaminations or misidentification of optical SNRs.

The total integrated H α line flux density from 26 SNRs from Blair & Long (1997) is 2.76×10^{-13} erg cm^{-2} s^{-1}.

3.10 NGC 4449

NGC 4449 is a Magellanic-type irregular galaxy with several areas of recent star formation, including the nucleus and the bar. This galaxy is known for an extensively studied Cas A-like SNR, which has been observed at all wavelengths (optical: Balick & Heckman 1978; Blair, Kirshner & Winkler 1983; X-rays: Patnaude & Fesen 2003; radio: Seaquist & Bignell 1978; Lacey, Goss & Mizouni 2007). This SNR was the only known optical SNR in NGC 4449 until recently, when Leonidaki et al. (2013) detected an additional 69 optical candidate SNRs. In the radio domain, Chomiuk & Wilcots (2009) detected seven new SNRs, which had all also been detected optically by Leonidaki et al. (2013). Using X-rays, Summers et al. (2003) observed NGC 4449 with the *Chandra* observatory, and they

suggested two sources to be SNRs, while the other eight were classified as SNR/X-ray binaries. Using the same *Chandra* observations, Leonidaki et al. (2010) suggested that four objects were SNRs or SNR candidates. All these four objects were also detected as optical SNR candidates (Leonidaki et al. 2013).

The total H α line flux density of 70 optical SNRs detected by Leonidaki et al. (2013) in NGC 4449 is 1.19×10^{-12} erg cm^{-2} s^{-1}.

3.11 M83

M83 is a grand-design spiral galaxy, with a starburst nucleus and active star formation. Its almost face-on orientation gives us a detailed view of star formation and destruction. It had six SNe in the last century, which makes it second only to NGC 6946. We should not be surprised that this galaxy has the highest number of optically detected SNR candidates. Blair & Long (2004) were the first to search for optical SNRs in M83. They made observations using the 4-m Blanco Telescope at the Cerro Tololo Inter-American Observatory and found 71 candidate SNRs. They also searched for X-ray counterparts to the optical detections by Soria & Wu (2003) and found 15 position matches. Two years later, Maddox et al. (2006) published VLA observations of M83; they found four sources that matched optical SNRs from Blair & Long (2004). Later, Dopita et al. (2010), using the Wide Field Camera on *HST*, detected 60 SNRs in one field of view. Of those 60 SNRs, one is a historical remnant, 40 were detected classically using the [S II]/H α ratio in the disc region of M83, while the other 19 were detected in the nuclear region ($R < 300$ pc). SNRs in the nucleus were detected using an enhanced [O II] line, and for only four were H α fluxes measured. Dopita et al. (2010) detected 12 SNRs from Blair & Long (2004). The largest contribution to the number of observed optical SNRs in M83 was made by Blair et al. (2012) (see also the erratum to that paper by Blair, Winkler & Long 2013). They observed the full extent of the galaxy, using the Magellan I 6.5-m Telescope under conditions of excellent seeing and with extremely deep exposures of 70 min. They detected 225 ISM-dominated SNRs in M83, using the [S II]/H α ratio technique, with an additional 33 [O III] selected objects, which could be candidates for ejecta-dominated SNRs. They confirmed all but three SNRs from Blair & Long (2004), and 25 out of 40 disc SNRs from Dopita et al. (2010). Blair et al. (2012) also searched for X-ray counterparts to their optical SNRs, and found that 65 of 225 ISM-dominated SNRs have X-ray counterparts, as well as five ejecta-dominated SNRs. Recently, Blair et al. (2014) presented an expanded *HST* survey of M83. They detected 26 new SNRs. In all three papers (Blair & Long 2004; Dopita et al. 2010; Blair et al. 2012, 2014), an extensive analysis of the physical and statistical parameters of the SNRs in M83 is given.

In M83, 296 SNRs have measured H α fluxes: 225 ISM-dominated and 33 ejecta-dominated SNRs from Blair et al. 2012; 12 disc and four nuclear SNRs from Dopita et al. (2010), which were not detected by Blair et al. (2012); and 22 from Blair et al. (2014). The total H α flux from these SNRs is 6.39×10^{-12} erg cm^{-2} s^{-1}.

3.12 NGC 4395

NGC 4395 is a nearby irregular starburst galaxy, hosting the least luminous Seyfert nucleus. This galaxy may host one radio candidate SNR, based on its non-thermal radio spectrum from VLA observations (Sramek 1992; Vukotić et al. 2005) and because of its positional coincidence with a H II region from Roy et al. (1996). Unfortunately, this object was not in the *Chandra* field for which Leonidaki et al. (2010) suggested two X-ray SNRs. At optical wavelengths, Leonidaki et al. (2013) found 47 candidate SNRs, although their observations did not cover the full extent of the galaxy. Among these detections there was one X-ray candidate (from Leonidaki et al. 2010), while the other was out of the field of view. The only radio candidate SNR in this galaxy was also detected, but it had [S II]/H $\alpha < 0.3$.

The total H α line flux density of 47 optical SNRs detected by Leonidaki et al. (2013) in NGC 4395 is 2.66×10^{-13} erg cm^{-2} s^{-1}.

3.13 NGC 5204

NGC 5204 is a nearby Magellanic-type galaxy, a member of the M101 Group of galaxies. In the literature, most studies have focused on the ULX source NGC 5204 X-1, close to the centre of the galaxy and its optical counterpart. In this galaxy, there have been only optical SNR detections. First, Matonick & Fesen (1997) detected three optical SNR candidates, and recently Leonidaki et al. (2013) confirmed these three detections and added 33 possible new SNRs. At X-ray wavelengths, Leonidaki et al. (2010) searched through archival *Chandra* images for SNRs in this galaxy, but they found no such candidates.

The total H α line flux density of 36 optical SNRs detected by Leonidaki et al. (2013) in NGC 5204 is 2.32×10^{-13} erg cm^{-2} s^{-1}.

3.14 NGC 5585

NGC 5585 is a late-type spiral galaxy in the M101 Group. The only paper to discuss SNRs in this galaxy is Matonick & Fesen (1997). They found only five optical SNRs. Among these five SNRs, there is one interesting object, SNR 1, with extremely large dimensions – 200 × 90 pc. This candidate SNR is similar to the already mentioned microquasar S26 in NGC 7793, although it is half the size. Unfortunately, there have been no additional observations of this unusual object that could reveal its true nature.

The total integrated H α line flux density for five SNRs in NGC 5585 from Matonick & Fesen (1997) is 6.78×10^{-14} erg cm^{-2} s^{-1}.

3.15 NGC 6946

NGC 6946 is a nearby ($d = 5.9$ Mpc) late-type spiral galaxy hiding a mild starburst nucleus (Turner & Ho 1983). This galaxy could be interesting to search for SNRs because there have been nine historical SNe in this galaxy (Barbon et al. 2010). The first detected SNR in NGC 6946 was MF 16 (from Matonick & Fesen 1997) and the detection used the *ROSAT* X-ray observatory (Schlegel 1994) following optical observations by Blair & Fesen (1994). The first systematic search for SNRs was performed by Matonick & Fesen (1997) in optical wavelengths. They discovered 27 optical SNR candidates. The same year, Lacey, Duric & Goss (1997) published their VLA observations of NGC 6946, and suggested 37 objects as possible SNRs. More recently, Pannuti et al. (2007) found, using their *Chandra* observations, six X-ray counterparts to candidate radio SNRs, but no counterparts to the optical SNRs.

Due to its large dimensions (>100 pc) and its ultra-high X-ray luminosity, there hve been many papers debating the true nature of the MF 16 source. Blair, Fesen & Schlegel (2001), based on *HST* observations through narrow-band filters, suggested that this object could be a result of multiple SN explosions, close temporally and spatially. Based on *Chandra* observations, Roberts & Colbert (2003) suggested that the extraordinary X-ray luminosity of MF 16

arises from a black hole X-ray binary and that this object is a ULX source.

The total integrated H α line flux density from 26 SNRs in NGC 6946 from Matonick & Fesen (1997) is 1.28×10^{-13} erg cm^{-2} s^{-1}.

3.16 M101

M101 is a nearly face-on (∼22° inclination) giant spiral galaxy at a distance of 6.7 Mpc. This galaxy has been well studied for SNRs. The first major search for SNRs in M101 was performed by Matonick & Fesen (1997), who detected 93 SNRs. With five fields of view, they covered the full size of the galaxy. Before that, one candidate radio SNR in M101, NGC 5471B, a part of a giant H II region, was known (Skillman 1985; Sramek & Weedman 1986; Yang, Skillman & Sramek 1994). Afterwards, Pannuti et al. (2007) searched for X-ray counterparts to optically identified SNRs from Matonick & Fesen (1997). Their observations covered 44 SNRs, and they found that six of them are visible also at X-ray wavelengths. The latest paper on SNRs in M101 was by Franchetti et al. (2012), who used archival *HST* H α images for 55 of the 93 SNR candidates identified by Matonick & Fesen (1997) and conducted detailed analysis of their physical structure and nature. Also, they used a deep *Chandra* X-ray mosaic of M101 made by Kuntz & Snowden (2010) to search for X-ray emissions of SNR candidates and found that 21 of the 55 SNR candidates in their study have X-ray counterparts. They also checked if the remaining 38 SNRs from Matonick & Fesen (1997), which do not have *HST* images, radiate X-rays, and they found that 11 of them have X-ray counterparts. From *HST* images, they found that 10 objects, out of 55 SNRs from Matonick & Fesen (1997), are actually superbubbles, and another 10 are OB/H II associations. These 10 were excluded from the list of SNRs in M101.

Finally, to estimate the H α flux from SNRs in M101, we combined the results from Matonick & Fesen (1997) and Franchetti et al. (2012). We have taken H α fluxes for 38 SNRs from Matonick & Fesen (1997) and 35 SNRs from Franchetti et al. (2012). The total integrated H α line flux density for the 73 SNRs in M101 is 3.46×10^{-13} erg cm^{-2} s^{-1}.

3.17 M74

M74 (NGC 628) is a face-on spiral galaxy at a distance of 7.3 Mpc and is the brightest member of the small M74 Group of galaxies. This galaxy has been well studied for its star-forming properties (Leievre & Roy 2000; Elmegreen et al. 2006). M74 has also had three SN explosions in the last 12 yr. Sonbas et al. (2010) detected nine SNRs at optical wavelengths in this galaxy. Previously, M74 had been observed at X-ray wavelengths using *Chandra* and *XMM-Newton* data by Soria, Pian & Mazzali (2004). Sonbas et al. (2010) found three matches between their SNR candidates and X-ray sources from Soria et al. (2004).

The total integrated H α line flux density for nine SNRs in M74 from Sonbas et al. (2010) is 1.05×10^{-13} erg cm^{-2} s^{-1}.

3.18 NGC 2903

NGC 2903 is a late-type barred spiral galaxy at a distance of 8.9 Mpc. It is also known as a 'hotspot' galaxy, because of its numerous bright nuclear condensations (Sersic 1973), which are believed to be OB associations and clusters. The only search for SNRs in this galaxy was performed by Sonbas, Akuyz & Balman (2009). They detected five optical SNR candidates. Based on their subarcsecond-resolution VLA imaging of NGC 2903, Tsai et al. (2006) reported that one of the seven detected discrete radio sources could be an SNR.

The total integrated H α line flux density for five SNRs in NGC 2903 from Sonbas et al. (2009) is 5.88×10^{-14} erg cm^{-2} s^{-1}.

4 DISCUSSION

In the previous section we gave an overview of the optical detection of SNRs in nearby galaxies, as well as some indication of the detection of SNRs at other wavelengths. In our sample, we present 18 galaxies that have been surveyed for optical SNRs.

In Table 2 we give the number and total H α flux of optical SNRs in each galaxy in our sample. Kennicutt et al. (2008) published 'An H α imaging survey of galaxies in the local 11 Mpc volume', which provided us with the H α fluxes for the 18 galaxies in our sample, as presented in the table. The total H α flux of each galaxy can be used to estimate SFR (according to equation (1)). Fluxes from Kennicutt et al. (2008) are corrected for Galactic foreground extinction and [N II] contamination. In Table 2 we give values used in Kennicutt et al. (2008) for these corrections. We applied these same corrections for SNR fluxes taken from the literature. Where H α fluxes for SNRs in the original work have been previously corrected for Galactic foreground extinction and [N II] contamination, we recalculated them so they are corrected in the same manner as done by Kennicutt et al. (2008). To remove [N II] contamination from fluxes, we used the integrated [N II] λλ6548, 6583/H α ratio from Kennicutt et al. (2008) and the procedure presented in Vučetić et al. (2013), which takes into account the different filter transmittances at the position of each of these three emission lines. No internal extinction correction was made to any of the fluxes presented in this paper.

Table 2 shows that the percentage of H α emission originating from SNR contamination is within the range 0.1–13 per cent. From Column (11) of Table 2, we see that six out of the seven highest values in this column originate from the paper by Leonidaki et al. (2013), and are within the range 5–13 per cent. Such a high percentage of around 10 per cent is not a negligible source of error for the determined SFRs. The situation that six out of the seven highest values are from the same group of authors does introduce doubt about their plausibility. It could be that the source of the high efficiency in the detection of SNRs by Leonidaki et al. (2013) is because they used a somewhat milder [S II]/Hα > 0.3 criterion for SNR detection. This lower criterion was also used by Dopita et al. (2010). Also, Leonidaki et al. (2013) detected 150 SNRs in NGC 2403, while Matonick et al. (1997) detected only 35. When we compare the differences in telescopes and exposure times used by these two groups, it would expected that Matonick et al. (1997) can achieve twice the detection efficiency achieved by Leonidaki et al. (2013). Although, one should note that Matonick et al. (1997) used a stronger [S II]/Hα > 0.45 criterion.

The M83 galaxy has the third highest percentage of SNR H α emission contamination – 9 per cent. This galaxy boasts the largest number of optical SNRs (296), and is the best sampled for optical SNRs among all galaxies. This is not surprising, since M83 has been observed with the 4-m Blanco Telescope (Blair & Long 2004), with *HST* (Dopita et al. 2010; Blair et al. 2014) and with the Magellan I 6.5-m Telescope with very long exposures (Blair et al. 2012). For this reason, we think that the percentage for M83 would be somewhat closer to the real contribution of SNR emission to the total H α emission in spiral galaxies.

Table 2. Our sample of galaxies with optical SNRs. Column (1): Galaxy name, as in Table 1. Column (2): Number of optically detected SNRs in the galaxy, with determined H α fluxes. Column (3): Fraction of galactic angular extension that has been surveyed for optical SNRs. Column (4): H α flux of optically detected SNRs, corrected for Galactic foreground extinction and [N II] contamination by Kennicutt et al. (2008). Column (5): Fractional error of H α flux of optically detected SNRs, as reported in the literature. The rule (–) means that no error estimates were published. Column (6): H α luminosity of optically detected SNRs, corrected for Galactic foreground extinction and [N II] contamination as in Kennicutt et al. (2008). Column (7): The adopted integrated [N II] $\lambda\lambda$6548, 6583/H α ratio (sum of both components), used in Kennicutt et al. (2008). Column (8): *B* band Galactic foreground extinction, used in Kennicutt et al. (2008). Extinction in the H α band is calculated as $A_{H\alpha} = 0.6A_B$. Column (9): Integrated H α flux for the galaxy. The flux is calculated using the integrated H α luminosity and distance in tables 2 and 3 in Kennicutt et al. (2008). This flux is reported with median fractional error of 12 per cent. Column (10): Integrated H α luminosity for the galaxy. Column (11): Percentage of H α flux from the SNRs in comparison to total H α flux of the galaxy – *R*. Since SFR is directly proportional to the H α luminosity (and flux) (see equation 1), this percentage also represents the fractional error made when the H α flux from SNRs is not removed from the total H α flux of the galaxy. Column (12): Fractional error of *R*. This is the sum of fractional errors for the H α fluxes of SNRs and of the galaxy. Column (13): References from which H α fluxes of optically detected SNRs are taken.

Galaxy name	No. of optical SNRs	Fraction surveyed	F_{SNRs} (erg cm^{-2} s^{-1}) $\times 10^{-14}$	δF_{SNRs} (per cent)	L_{SNRs} (erg s^{-1}) $\times 10^{38}$	[N II]/H α ratio	A_B (mag)	F_{gal} (erg cm^{-2} s^{-1}) $\times 10^{-12}$	L_{gal} (erg s^{-1}) $\times 10^{39}$	R (per cent)	δR (per cent)	Ref.
(1)	(2)	(3)	(4)	(5)	(6)	(7)[a]	(8)[a]	(9)[a]	(10)[a]	(11)	(12)	(13)
M31	156	1	371.9	–	2.8	0.54	0.18	360.4	26.9	1.0	12	1
M33	137	1	544.6	–	4.6	0.27	0.18	383.0	32.4	1.4	12	2
NGC 300	22	1	23.1	22	1.1	0.2	0.06	31.6	15.1	0.7	34	3
NGC 4214	92	1	178.0	2	18.2	0.16	0.05	15.2	15.5	11.7	14	4
NGC 2403	150	0.88	620.7	1	77.0	0.29	0.17	48.6	60.3	12.8	13	4,5
M82	10	0.07	2.7	5	0.4	0.3	0.4	78.8	117.5	0.1	17	6
M81	41	1	18.8	–	3.0	0.51	0.24	37.3	58.9	0.5	12	7
NGC 3077	24	1	28.3	6	5.0	0.38	0.25	5.5	9.5	5.2	18	4
NGC 7793	27	1	28.8	–	5.3	0.25	0.08	20.8	38.0	1.4	12	8
NGC 4449	71	1	121.6	2	25.8	0.23	0.04	24.2	51.3	5.0	14	4
M83	296	1	653.0	–	156.0	0.53	0.21	74.4	177.8	8.8	12	9,10,11
NGC 4395	47	0.73	27.2	3	6.9	0.19	0.04	4.5	11.5	6.0	15	4
NGC 5204	36	1	23.6	4	6.1	0.13	0.03	3.1	8.1	7.5	16	4
NGC 5585	5	1	6.9	–	2.7	0.18	0.03	2.1	8.1	3.3	12	7
NGC 6946	26	0.95	12.1	–	5.0	0.54	1.54	69.2	288.4	0.2	12	7
M101	73	0.98	35.0	–	19.2	0.54	0.02	39.8	213.8	0.8	12	7,12
M74	9	0.83	9.4	–	6.0	0.4	0.21	11.6	74.1	0.8	12	13
NGC 2903	5	1	4.9	–	4.6	0.56	0.1	12.4	117.5	0.4	12	14

[a]From Kennicutt et al. (2008).

REFERENCES: (1) Lee & Lee (2014); (2) Long et al. (2010); (3) Millar et al. (2011); (4) Leonidaki et al. (2013); (5) Matonick et al. (1997); (6) de Grijs et al. (2000); (7) Matonick & Fesen (1997); (8) Blair & Long 1997); (9) Dopita et al. (2010); (10) Blair et al. (2013); (11) Blair et al. (2014); (12) Franchetti et al. (2012); (13) Sonbas et al. (2010); (14) Sonbas et al. (2009).

We emphasize that in our estimates of the H α fluxes from SNRs in each galaxy, we have taken fluxes from both confirmed SNRs (confirmed either spectroscopically or by observations at other wavelengths) and SNR candidates, which have been classified only upon the [S II]/H α ratio criterion. This could lead to an overestimation of the percentage *R*, considering that there might be numerous false identifications of SNR candidates.

In Column (3) of Table 2, we present the fraction of the angular extension of a galaxy covered by observations for optical SNRs. The majority of galaxies have been fully covered, four of the rest have been more than 80 per cent covered, while the M82 galaxy has had only a small fraction of its disc observed for SNRs. For galaxies that have not been fully observed, only the outer parts of the galactic surface have not been covered. If we assume that SNe follow the radial distribution of gas and dust in a galaxy (Hatano, Branch & Deaton 1998), then we would expect that the number of SNe, as well as the number of SNRs, will rapidly decrease as we move away from the galactic centre. In this context, as only the outer parts of galaxies have not been observed, we do not expect a major change in the number of SNRs and their total H α flux if the whole galactic surfaces were to be observed. For only M82 would the change be significant, but due to the large internal extinction in that galaxy, it is hard to estimate the number of SNRs that would be detected in the galaxy as a whole.

Another very important question which we discuss here is how we can compare data collected in very different studies, with different flux sensitivities and from different galaxies.

To discuss the completeness of the samples, we have to assume some number distribution function of SNRs with respect to flux or luminosity – we shall choose luminosity so that we can compare different samples. If this distribution is log-normal, i.e. normal or Gaussian in the logarithmic scale:

$$F(L) = \frac{N^*}{\sigma\sqrt{2\pi}} \mathrm{e}^{-(\ln L - \mu)^2/(2\sigma^2)},$$

then from the fit we can estimate the number of missing SNRs as $N^\star - N$, where $N^\star$ and N are the corrected and detected number of SNRs, and their contribution to the total H α luminosity. $\mu = \ln L_m$ is the natural logarithm of luminosity, which corresponds to the maximum of the distribution, i.e. the mean, and σ is the standard deviation of the normal distribution.

It is usually assumed that a sample is complete for high fluxes (or luminosities) up to the maximum (Matonick & Fesen 1997; Leonidaki et al. 2013). While it is quite likely that we will detect all bright and luminous objects, we can still miss the extended low surface-brightness (and thereby luminous) SNRs. However, we will assume that these are rare.

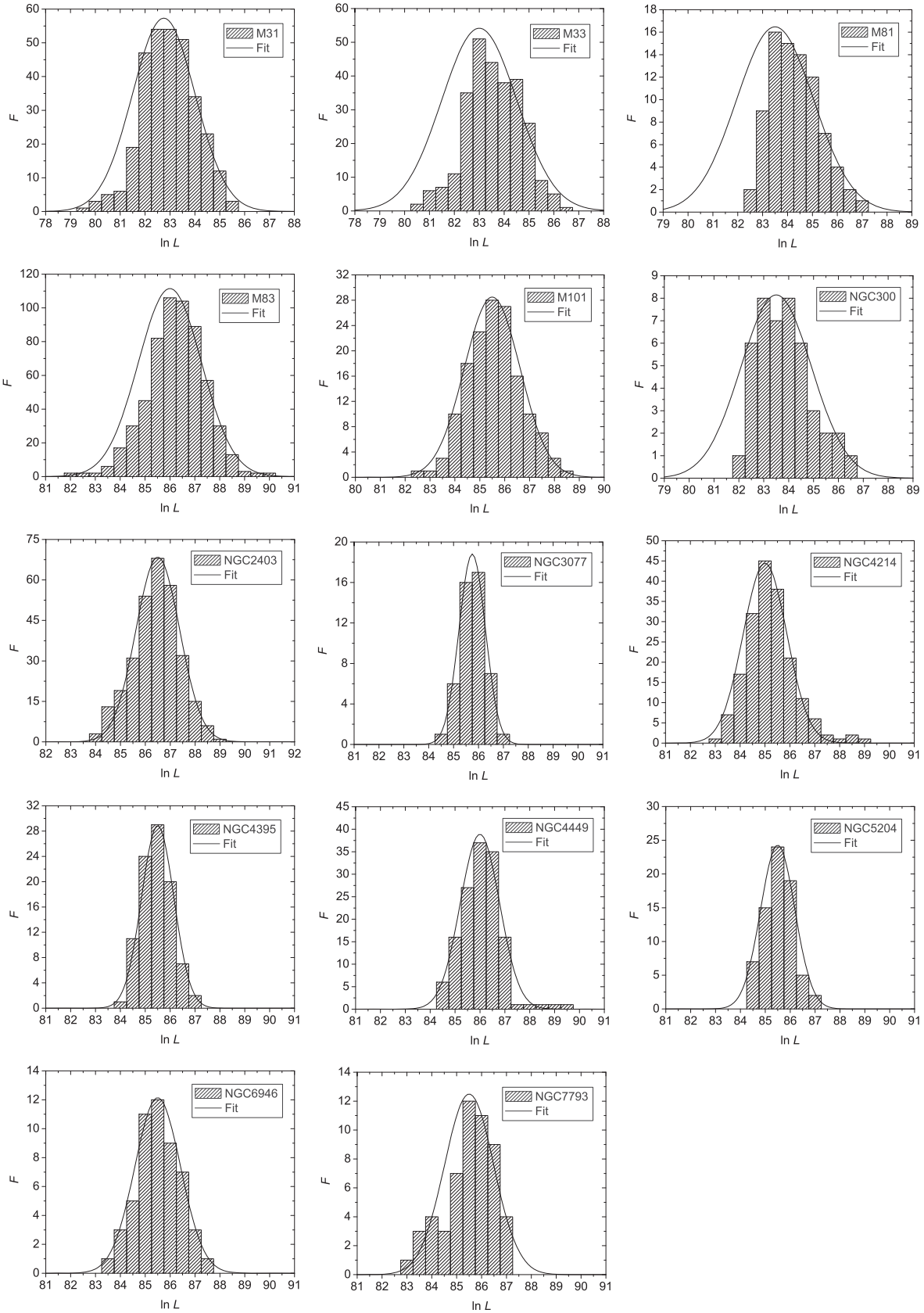

Figure 1. Number distributions of SNRs for our galaxy sample and fitted normal distributions.

Table 3. Basic properties and corrected parameters of number distributions of SNRs in our galaxy sample. N is the number of detected SNRs in each galaxy. $N^\star$ and $\Delta N^\star$ are the corrected number and error from the Gaussian fit. L_o is the minimum luminosity observed and L_m is the luminosity corresponding to the maximum of the distribution. σ and $\Delta\sigma$ are the standard deviation of the normal distribution and error. L_{SNRs} is the measured total luminosity of the SNRs. $L^\star$ is the corrected total luminosity of the SNRs. R and $R^\star$ are the ratio and the corrected ratio of H α luminosity from the SNRs to the total H α luminosity of the galaxy.

Galaxy	N	$N^\star$	$\Delta N^\star$	$\ln L_o$	$\ln L_m$	σ	$\Delta\sigma$	L_{SNRs} (erg s^{-1})	$L^\star$ (erg s^{-1})	R	$R^\star$
M31	156	181	6	79.51	82.75	1.26	0.05	2.76×10^{38}	3.47×10^{38}	1.03	1.29
M33	137	205	15	80.53	83	1.51	0.11	4.60×10^{38}	7.13×10^{38}	1.42	2.20
M81	41	64	3	82.89	83.5	1.55	0.07	2.99×10^{38}	3.90×10^{38}	0.50	0.66
M83	296	355	10	82.12	86	1.27	0.07	1.56×10^{40}	1.78×10^{40}	8.78	10.00
M101	73	80	4	82.61	85.5	1.12	0.05	1.91×10^{39}	2.03×10^{39}	0.88	0.95
NGC 300	22	29	2	82.43	83.5	1.42	0.09	1.11×10^{38}	1.46×10^{38}	0.73	0.96
NGC 2403	150	151	3	84.06	86.5	0.88	0.03	7.71×10^{39}	8.20×10^{39}	12.77	13.60
NGC 3077	24	25	1	84.87	85.75	0.53	0.01	4.96×10^{38}	5.01×10^{38}	5.18	5.24
NGC 4214	92	98	4	83.28	85	0.88	0.04	1.82×10^{39}	1.19×10^{39}	11.71	7.66
NGC 4395	47	47	2	84.25	85.5	0.65	0.02	6.88×10^{38}	7.87×10^{38}	6.02	6.86
NGC 4449	71	77	6	84.73	86	0.79	0.08	2.57×10^{39}	2.35×10^{39}	5.03	4.58
NGC 5204	36	42	2	84.56	85.5	0.69	0.03	6.12×10^{38}	7.22×10^{38}	7.50	8.89
NGC 6946	26	28	1	83.63	85.5	0.92	0.03	5.05×10^{38}	5.80×10^{38}	0.17	0.20
NGC 7793	27	31	4	83.42	85.5	0.99	0.11	5.30×10^{38}	6.86×10^{38}	1.39	1.80

We have thus fitted only the right-hand side of the observed distributions, excluding local minima and bars that are lower than their left-hand side counterparts, and keeping the mean, i.e. $\ln L_m$, fixed. We could do this only for the 14 galaxies from our sample that have sufficient SNRs detected to give the distribution of the number of SNRs over luminosity. The results are given in Fig. 1 and Table 3. When the fitted parameters $N^\star$ and σ have been found, we can obtain the corrected total luminosity of SNRs, which is actually the mean of the log-normal distribution

$$L^* = \int_0^\infty Lf(L)\mathrm{d}L = N^* \cdot \mathrm{e}^{\mu+\sigma^2/2}, \quad (2)$$

where

$$f(L) = \frac{N^*}{\sigma\sqrt{2\pi}L}\mathrm{e}^{-(\ln L-\mu)^2/(2\sigma^2)}.$$

Now we can also obtain the ratio of H α luminosity from the SNRs to the total H α luminosity of the galaxy, which is corrected for possible incompleteness of the SNR sample – $R^\star$. If we compare the uncorrected R and corrected $R^\star$ (from Table 3) we can see that the biggest change in values is for the M33 and NGC 4214 galaxies, but the highest value of 13 per cent of SNR contamination is not changed.

We can see that, according to the fit, only for galaxies M33, M81 and NGC 300 is there a significant number of low luminous SNRs missing. However, because of the characteristics of a log-normal distribution, $L^\star$ is not very different from the uncorrected total H α luminosity of SNRs, neither for these three nor for all other galaxies. For two galaxies, NGC 4214 and NGC 4449, $L^\star$ is slightly smaller than L_{SNRs}, which is due to the existence of very bright SNRs in these galaxies, i.e. the distribution cannot be approximated with a single Gaussian.

Even if the real distribution over luminosities is indeed Gaussian (in the logarithmic scale), which may be an overly simplistic assumption because of the selection effects and sensitivity limits, the observed mean, i.e. the logarithm of luminosity, which corresponds to the maximum of the distribution $\ln L_m$, may not be the true mean μ, which in reality may be shifted to lower luminosities. In principle, we may expect that if the sensitivity limit, i.e. the minimum luminosity L_o, is far from L_m, the mode, i.e. mean, is well determined. To test this, for spirals we looked for a possible correlation between the corrected ratio of H α luminosity from the SNRs to the total H α luminosity of the galaxy $R^\star$ and $\ln(L_m/L_o)$ – galaxies with high $\ln(L_m/L_o)$ should then have a more reliable (and higher) R. However, no evident correlation can be seen from Fig. 2 . We also checked for any correlation between $R^\star$ and galaxy properties (inclination and galaxy type), but again without much success (Figs 3 and 4).

4.1 SNR contamination and SN type

We assume that the remnants of type Ia SNe are not as easily detectable as those of type II or Ib/c. Type Ia SNe have a possible tendency to occur in the low-density regions of a galaxy and leave no optically detectable remnants. Similarly, Balmer-dominated SNRs, which are thought to be related to type Ia SNe (van den Bergh 1988), will be missed by optical searches using the [S II]/H $\alpha > 0.4$ criterion. A study of the SN rate by Mannucci et al. (2005) found that it is about 25 per cent for type Ia explosions in spiral and irregular galaxies. This is in good agreement with Lee & Lee (2014), who suppose that 23 per cent of all optical SNRs in M31 originated from type Ia events. Furthermore, Braun & Walterbos (1993) estimated that about half of all core-collapse SNe (type II or Ib/c), will happen in associations and leave no detectable remnant. With these assumptions, we would be able to detect optically only about one-third of all SNRs. This is because only a few SNRs are observed inside H II regions and because optical searches appear to be biased against detecting large and faint SNRs. Although SNRs are rarely detected inside H II regions and stellar associations, there must certainly be SNRs inside such objects (remnants of type II and Ib/c SNe). There is evidence that SNRs are often associated with giant H II regions, such as 30 Doradus (the giant H II region in the LMC) (Ye 1988), the SMC (Ye, Turtle & Kennicutt 1991) and NGC 4449 (Kirshner & Blair 1980). Even though SNRs embedded in an H II region are not separated from the associated region, we expect that there must be

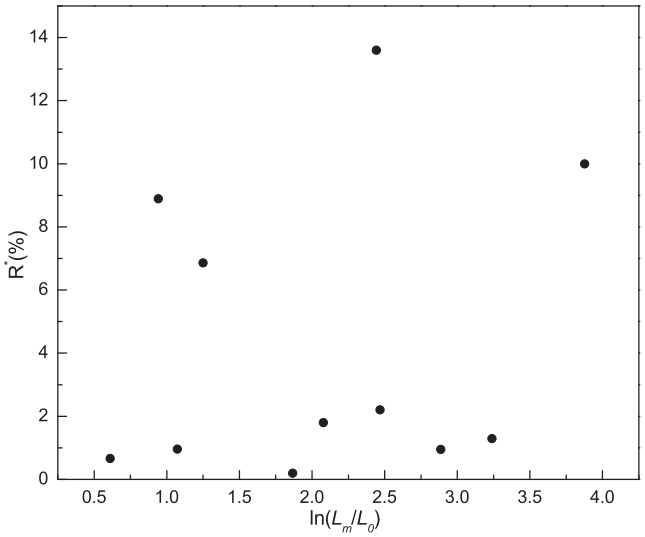

Figure 2. Plot of corrected ratio of H α luminosity from the SNRs to the total H α luminosity of the galaxy $R^{\star}$ versus ln $(L_{\rm m}/L_{\rm o})$ for 11 spiral galaxies from our sample. $L_{\rm m}$ is the luminosity corresponding to the maximum of the SNR number distribution and $L_{\rm o}$ is the sensitivity limit, i.e. the minimum luminosity. There is no correlation.

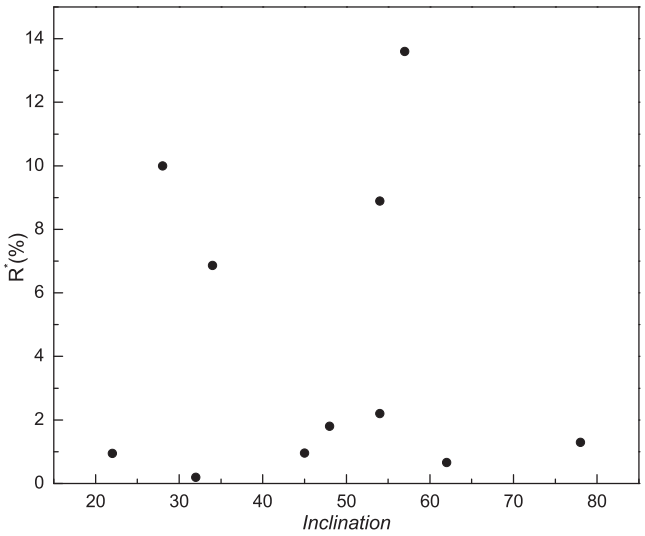

Figure 3. Plot of corrected ratio of H α luminosity from the SNRs to the total H α luminosity of the galaxy $R^{\star}$ versus galaxy inclination for 11 spiral galaxies from our sample. There is no correlation.

some contribution from such SNRs to the total H α radiation, which should increase the influence of SNR contamination on SFRs.

The selection effects that affect detection of SNRs are related to an observational fact that the optical SNRs on average lie in regions of lower gas density. Due to this they are biased against star-forming regions, which typically tend to have higher than average gas density (for details of this observational bias see Pannuti et al. 2000). Taking this into account, we emphasize that the derived percentages for H α emission from the SNRs to the total H α fluxes used to estimate SFRs in the galaxies are only a lower limit.

5 CONCLUSIONS

Out of 25 nearby galaxies with observed SNRs in the optical range, we have presented details of SNR detection for our sample of 18

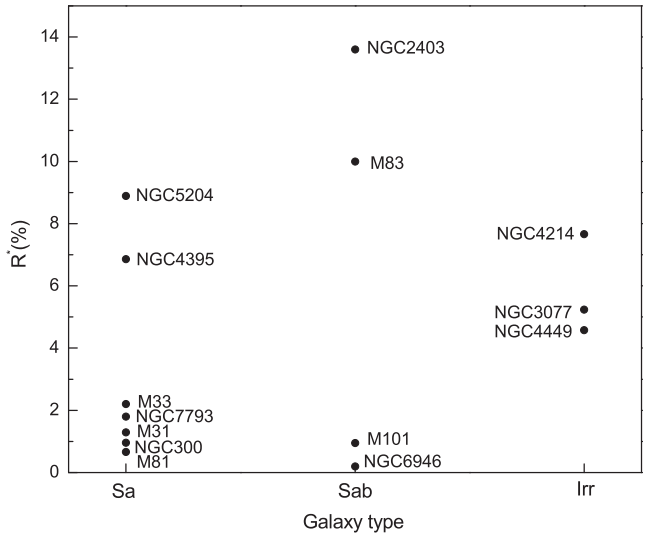

Figure 4. Dependence of corrected ratio of H α luminosity from the SNRs to the total H α luminosity of the galaxy $R^{\star}$ on galaxy type.

galaxies. We have discussed the contribution of the H α fluxes from the SNRs to the total H α flux and its influence on the derived SFR for each galaxy in the sample. We have found that the average SNR contamination of the total H α flux and derived SFRs for the nearby galaxies analysed is 5 ± 5 per cent. The highest SNR contamination is about 13 per cent. The M83 galaxy is the best sampled for optical SNRs and SNRs account for 9 per cent of the total H α emission. We expect that percentages similar to this would be close to the real contribution of SNR emission to the total H α emission in spiral galaxies. Due to selection effects, the SNR H α contamination obtained in this paper is only a lower limit.

ACKNOWLEDGEMENTS

We are grateful to Miroslav Filipović for useful comments and suggestions, Dragana Momić for careful reading and correction of the manuscript and to the anonymous referee for a comprehensive report that helped us improve it significantly. This research has been supported by the Ministry of Education, Science and Technological Development of the Republic of Serbia through project No. 176005 'Emission nebulae: structure and evolution' and it is a part of a joint project btween the Serbian Academy of Sciences and Arts and the Bulgarian Academy of Sciences 'Optical search for supernova remnants and H II regions in nearby galaxies (M81 group and IC342)'. This research has made use of the NASA/IPAC Extragalactic Database (NED), which is operated by the Jet Propulsion Laboratory, California Institute of Technology, under contract with NASA, and NASA's Astrophysics Data System Bibliographic Services.

REFERENCES

Abolmasov P., Fabrika S., Sholukhova O., Afanasiev V., 2007, Astrophys. Bull., 62, 36
Adelman-McCarthy J. K. et al., 2006, ApJS, 162, 38
Andjelić M. M., 2011, Serbian Astron. J., 183, 71
Andjelić M., Stavrev K., Arbutina B., Ilić D., Urošević D., 2011, Balt. Astron., 20, 459
Arbutina B., Ilić D., Stavrev K., Urošević D., Vukotić B., Onić D., 2009, Serbian Astron. J., 179, 87
Azimlu M., Marciniak R., Barmby P., 2011, AJ, 87, 1165

Badenes C., Maoz D., Draine B. T., 2010, MNRAS, 407, 1301
Balick B., Heckman T., 1978, ApJ, 226, L7
Barbon R., Buondi V., Cappellaro E., Turatto M., 2010, VizieR Online Data Catalog 102024
Bechtold J., Yee H. K. C., Elston R., Ellingson E., 1997, ApJ, 477, L29
Blair W. P., Fesen R. A., 1994, ApJ, 424, 103
Blair W. P., Long K. S., 1997, ApJS, 108, 261
Blair W. P., Long K. S., 2004, ApJS, 155, 101
Blair W. P., Kirshner R. P., Chevalier R. A., 1981, ApJ, 247, 879
Blair W. P., Kirshner R. P., Winkler P. F., 1983, ApJ, 272, 84
Blair W. P., Fesen R. A., Schlegel E. M., 2001, AJ, 121, 1497
Blair W. P., Winkler P. F., Long K. S., 2012, ApJS, 203, 8
Blair W. P., Winkler P. F., Long K. S., 2013, ApJS, 207, 40
Blair W. P. et al., 2014, ApJ, 788, 55
Bozzetto L. M. et al., 2012a, MNRAS, 420, 2588
Bozzetto L. M., Filipović M. D., Crawford E. J., De Horta A. Y., Stupar M., 2012b, Serbian Astron. J., 184, 69
Bozzetto L. M., Filipović M. D., Urošević D., Crawford E. J., 2012c, Serbian Astron. J., 185, 25
Bozzetto L. M. et al., 2013, MNRAS, 432, 2177
Bozzetto L. M. et al., 2014, MNRAS, 439, 1110
Braun R., Walterbos R. A. M., 1993, A&AS, 98, 327
Butler D. J., Martínez-Delgado D., Brandner W., 2004, AJ, 127, 1472
Čajko K. O., Crawford E. J., Filipović M. D., 2009, Serbian Astron. J., 179, 55
Chomiuk L., Wilcots E. M., 2009, AJ, 137, 3869
Conn A. R. et al., 2012, ApJ, 758, 11
D'Odorico S., Dopita M. A., 1983, in Proc. Symp., Supernova Remnants and Their X-ray Emission. D. Reidel Publishing Co., Dordrecht, p. 517
D'Odorico S., Dopita M. A., Benvenuti P., 1980, A&AS, 40, 67
de Grijs R., O'Connell R. W., Becker G. D., Chevalier R. A., Gallagher J. S., 2000, AJ, 119, 681
de Horta A. Y. et al., 2012, A&A, 540, 25
Dickel J. R., D'Odorico S., 1984, MNRAS, 206, 351
Dickel J. R., D'Odorico S., Felli M., Dopita M. A., 1982, ApJ, 252, 582
Donas J., Deharveng J. M., 1984, A&A, 140, 325
Dopita M. A. et al., 2010a, ApJ, 710, 964
Dopita M. A. et al., 2010b, Ap&SS, 330, 123
Dopita M. A., Payne J. L., Filipović M. D., Pannuti T. G., 2012, MNRAS, 427, 956
Drozdovsky I. O., Karachentsev I. D., 2000, A&AS, 142, 425
Eck C. R., Cowan J. J., Branch D., 2002, ApJ, 573, 306
Elmegreen B. G., Elmegreen D. M., Chandar R., Whitmore B., Regan M., 2006, ApJ, 644, 879
Fabbiano G., 1988, ApJ, 325, 544
Fenech D. M., Muxlow T. W. B., Beswick R. J., Pedlar A., Argo M. K., 2008, MNRAS, 391, 1384
Fenech D. M., Beswick R. J., Muxlow T. W. B., Pedlar A., Argo M. K., 2010, MNRAS, 408, 607
Feng H., Kaaret P., 2008, ApJ, 675, 1067
Ferguson A. M. N., Wyse R. F. G., Gallagher J. S., Hunter D. A., 1996, AJ, 111, 2265
Ferrerese L. et al., 2000, ApJS, 128, 431
Filipović M. D., Haynes R. F., White G. L., Jones P. A., 1998, A&AS, 130, 421
Filipović M. D., Payne J. L., Reid W., Danforth C. W., Staveley-Smith L., Jones P. A., White G. L., 2005, MNRAS, 364, 217
Fossey J., Cooke B., Pollack G., Wilde M., Wright T., 2014, Cent. Bureau Electron. Telegrams, 3792, 1
Franchetti N. A. et al., 2012, AJ, 143, 85
Freedman W. L. et al., 2001, ApJ, 553, 47
Gallagher J. S., III, Hunter D. A., Mould J. R., 1984, ApJ, 281, L63
Garn T. et al., 2010, MNRAS, 402, 2007
Geach J. E., Smail I., Best P. N., Kurk J., Casali M., Ivison R. J., Coppin K., 2008, MNRAS, 388, 1473
Gladstone J. C., Roberts T. P., Done C., 2009, MNRAS, 397, 1836
Gonçalves D. R., Magrini L., Martins L. P., Teodorescu A. M., Quireza C., 2012, MNRAS, 419, 854
Gordon S. M., Kirshner R. P., Long K. S., Blair W. P., Duric N., Smith R. C., 1998, ApJS, 117, 89
Gordon S. M., Duric N., Kirshner R. P., Goss W. M., Viallefond F., 1999, ApJS, 120, 247
Grisé F., Kaaret P., Pakull M. W., Motch C., 2011, ApJ, 734, 23
Haberl F. et al., 2012a, A&A, 543, 154
Haberl F. et al., 2012b, A&A, 545, 128
Hatano K., Branch D., Deaton J., 1998, ApJ, 502, 177
Hodge P. W., 1977, ApJS, 33, 69
Hopkins A. M., Beacom J. F., 2006, ApJ, 651, 142
Hopkins P. F., Quataert E., Murray N., 2011, MNRAS, 417, 950
Huang Z. P., Thuan T. X., Chevalier R. A., Condon J. J., Yin Q. F., 1994, ApJ, 424, 114
Huchra J. P., Geller M. J., Gallagher J., Hunter D., Hartmann L., Fabbiano G., Aaronson M., 1983, ApJ, 274, 125
James P. A., Shane N. S., Knapen J. H., Etherton J., Percival S. M., 2005, A&A, 429, 851
Karachentsev I. D., Kaisin S. S., 2007, ApJ, 133, 1883
Karachentsev I. D., Kopylov A. I., Kopylova F. G., 1994, Bull. Spectrosc. Astrophys. Obser., 38, 5
Karachentsev I. D. et al., 2002, A&A, 383, 125
Karachentsev I. D. et al., 2003a, A&A, 398, 479
Karachentsev I. D. et al., 2003b, A&A, 404, 93
Karachentsev I. D., Karachentseva V. E., Huchtmeier W. K., Makarov D. I., 2004, AJ, 127, 2031
Karim A. et al., 2011, ApJ, 730, 61
Kaufman M., Bash F. N., Kennicutt R. C., Hodge P. W., 1987, ApJ, 319, 61
Kennicutt R. C., 1983, ApJ, 272, 54
Kennicutt R. C., 1998, ARA&A, 36, 189
Kennicutt R. C., Evans N. J., 2012, ARA&A, 50, 531
Kennicutt R. C., Kent S. M., 1983, AJ, 88, 1094
Kennicutt R. C., Tamblyn P., Congdon C. E., 1994, ApJ, 435, 22
Kennicutt R. C., Lee J. C., Funes J. G., Sakai S., Akiyama S., 2008, ApJS, 178, 247
Kennicutt R. C. et al., 2009, ApJ, 703, 1672
Kirshner R. P., Blair W. P., 1980, ApJ, 236, 135
Kong A. K. H., Sjouwerman L. O., Williams B. F., Garcia M. R., Dickel J. R., 2003, ApJ, 590, L21
Kong A. K. H., Sjouwerman L. O., Williams B. F., 2004, ApJ, 128, 2783
Kronberg P. P., Wilkinson P. N., 1975, ApJ, 200, 430
Kronberg P. P., Biermann P., Schwab F. R., 1985, ApJ, 291, 693
Kumar C. K., 1976, PASP, 88, 323
Kuntz K. D., Snowden S. L., 2010, ApJS, 188, 46
Lacey C. K., Duric N., Goss W. M., 1997, ApJS, 109, 417
Lacey C. K., Goss W. M., Mizouni L. K., 2007, AJ, 133, 2156
Lee J. H., Lee M. G., 2014, ApJ, 786, 130
Leievre M., Roy J. R., 2000, ApJ, 120, 1306
Lenc E., Tingay S. J., 2006, AJ, 132, 1333
Leonidaki I., Zezas A., Boumis P., 2010, ApJ, 725, 842
Leonidaki I., Boumis P., Zezas A., 2013, MNRAS, 429, 189
Long K. S. et al., 2010, ApJS, 187, 495
Lozinskaya T. A., Silchenko O. K., Helfand D. J., Goss W. M., 1998, AJ, 116, 2328
Maddox L. A., Cowan J. J., Kilgard R. E., Lacey C. K., Prestwich A. H., Stockdale C. J., Wolfing E., 2006, AJ, 132, 310
Maggi P. et al., 2012, A&A, 546, 109
Magnier E. A., Prins S., van Paradijs J., Lewin W. H. G., Supper R., Hasinger G., Pietsch W., Trumper J., 1995, A&AS, 114, 215
Mannucci F., Della Valle M., Panagia N., Cappellaro E., Cresci G., Maiolino R., Petrosian A., Turatto M., 2005, A&A, 433, 807
Markoff S. et al., 2008, ApJ, 681, 905
Martínez-Delgado D., Aparicio A., Gallart C., 1999, AJ, 118, 2229
Massey P., Olsen K. A. G., Hodge P. W., Strong S. B., Jacoby G. H., Schlingman W., Smith R. C., 2006, AJ, 131, 2478
Mathewson D. S., Clarke J. N., 1972, ApJ, 178, L107
Mathewson D. S., Clarke J. N., 1973a, ApJ, 180, 725

Mathewson D. S., Clarke J. N., 1973b, ApJ, 182, 697
Mathewson D. S., Ford V. L., Dopita M. A., Tuohy I. R., Long K. S., Helfand D. J., 1983, ApJS, 51, 345
Mathewson D. S., Ford V. L., Dopita M. A., Tuohy I. R., Mills B. Y., Turtle A. J., 1984, ApJS, 55, 189
Mathewson D. S., Ford V. L., Tuohy I. R., Mills B. Y., Turtle A. J., Helfand D. J., 1985, ApJS, 58, 197
Matonick D. M., Fesen R. A., 1997, ApJS, 112, 49
Matonick D. M., Fesen R. A., Blair W. P., Long K. S., 1997, ApJS, 113, 333
Millar W. C., White G. L., Filipović M. D., Payne J. L., Crawford E. J., Pannuti T. G., Staggs W. D., 2011, Ap&SS, 332, 221
Moon D., Harrison F. A., Cenko S. B., Shariff J. A., 2011, ApJ, 731, L32
Murphy Williams R. N., Dickel J. R., Chu Y., Points S., Winkler F., Johnson M., Lodder K., 2010, Bull. American Astron. Soc., 41, 470
Muxlow T. W. B., Pedlar A., Wilkinson P. N., Axon D. J., Sanders E. M., de Bruyn A. G., 1994, MNRAS, 266, 455
Oey M. S., Kennicutt R. C., 1997, MNRAS, 291, 827
Ott J., Martin C. L., Walter F., 2003, ApJ, 594, 776
Pakull M. W., Soria R., Motch C., 2010, Nature, 466, 209
Pannuti T. G., Duric N., Lacey C. K., Goss W. M., Hoopes C. G., Walterbos R. A. M., Magnor M. A., 2000, ApJ, 544, 780
Pannuti T. G., Duric N., Lacey C. K., Ferguson A. M. N., Magnor M. A., Mendelowitz C., 2002, ApJ, 565, 966
Pannuti T. G., Schlegel E. M., Lacey C. K., 2007, AJ, 133, 1361
Pannuti T. G., Schlegel E. M., Filipović M. D., Payne J. L., Petre R., Harrus I. M., Staggs W. D., Lacey C. K., 2011, AJ, 142, 20
Patnaude D. J., Fesen R. A., 2003, ApJ, 587, 221
Payne J. L., Filipović M. D., Pannuti T. G., Jones P. A., Duric N., White G. L., Carpano S., 2004, A&A, 425, 443
Payne J. L., White G. L., Filipović M. D., Pannuti T. G., 2007, MNRAS, 376, 1793
Payne J. L., White G. L., Filipović M. D., 2008, MNRAS, 383, 1175
Peimbert M., Bohigas J., Torres-Peimbert S., 1988, Rev. Mexican Astron. Astrofis, 16, 45
Pietsch W., Freyberg M., Haberl F., 2005, A&A, 434, 483
Plucinsky P. P. et al., 2008, ApJS, 174, 366
Rieke G. H., Lebofsky M. J., 1978, ApJ, 220, L37
Roberts T. P., Colbert E. J. M., 2003, MNRAS, 341, 49
Roberts T. P., Goad M. R., Ward M. J., Warwick R. S., 2003, MNRAS, 342, 709
Rosa-Gonzalez D., 2005, MNRAS, 364, 1304
Roy J.-R., Belley J., Dutil Y., Martin P., 1996, ApJ, 460, 284.
Saha A., Claver J., Hoessel J. G., 2002, AJ., 124, 839
Sakai S., Madore B. F., 1999, ApJ, 526, 599
Salpeter E. E., 1955, ApJ, 121, 161
Sandage A. R., 1971, ApJ, 166, 13
Sasaki M., Pietsch W., Haberl F., Hatzidimitriou D., Stiele H., Williams B. F., Kong A. K. H., Kolb U., 2012, A&A, 544, 144
Schlegel M., 1994, ApJ, 424, 99
Seaquist E. R., Bignell R. C., 1978, ApJ, 226, L5
Searle L., Sargent W. L. W., Bagnuolo W. G., 1973, ApJ, 179, 427
Sersic J. L., 1973, PASP, 85, 103
Sharina M. E., Karachentsev I. D., Tikhonov N. A., 1996, A&AS, 119, 499
Skillman E. D., 1985, ApJ, 290, 449
Smith C., Leiton R., Pizarro S., 2000, in Alloin D., Olsen K., Galaz G., eds, ASP Conf. Ser. Vol. 221, Stars, Gas and Dust in Galaxies: Exploring the Links. Astron. Soc. Pac., San Francisco, p. 83
Sobral D., Best P. N., Matsuda Y., Smail I., Geach J. E., Cirasuolo M., 2012, MNRAS, 420, 1926
Sobral D., Smail I., Best P. N., Geach J. E., Matsuda Y., Stott J. P., Cirasuolo M., Kurk J., 2013, MNRAS, 428, 1128
Sonbas E., Akyuz A., Balman S., 2009, A&A, 493, 1061
Sonbas E., Akyuz A., Balman S., Özel M. E., 2010, A&A, 517, 91
Soria R., Wu K., 2003, A&A, 410, 53
Soria R., Pian E., Mazzali P. A., 2004, A&A, 413, 107
Soria R., Pakull M., Broderick J., Corbel S., Motch C., 2010, AIP Conf. Proc., 1248, 127
Sramek R., 1992, in Filipenko A. V., ed., ASP Conf. Ser. Vol. 31, Relationships Between Active Galactic Nuclei and Starburst Galaxies. Astron. Soc. Pac., San Francisco, p. 273
Sramek R. A., Weedman D. W., 1986, ApJ, 302, 640S
Stiele H., Pietsch W., Haberl F., Hatzidimitriou D., Barnard R., Williams B. F., Kong A. K. H., Kolb U., 2011, A&A, 534, A55
Summers L. K., Stevens I. R., Strickland D. K., Heckman T. M., 2003, MNRAS, 342, 690
Supper R., Hasinger G., Lewin W. H. G., Magnier E. A., van Paradijs J., Pietsch W., Read A. M., Trumper J., 2001, A&A, 373, 63
Thim F., Tammann G. A., Saha A., Dolphin A., Sandage A., Tolstoy E., Labhardt L., 2003, ApJ, 590, 256
Tsai C.-W., Turner J. L., Beck S. C., Crosthwaite L. P., Ho P. T. P., Meier D. S., 2006, AJ, 132, 2383
Tully R., 1988, Nearby Galaxies Catalog. Cambridge Univ. Press, Cambridge
Tully R. B. et al., 2006, AJ, 132, 729
Turner J. L., Ho P. T. P., 1983, ApJ, 268, L79
Turner J. L., Ho P. T. P., 1994, ApJ, 421, 122
Ulvestad J. S., 2000, AJ, 120, 278
van den Bergh S., 1988, ApJ, 327, 156
van den Bergh S., 2000, PASP, 112, 529
van der Heyden K. J., Bleeker J. A. M., Kaastra J. S., 2004, A&A, 421, 1031
Villar V. et al., 2008, ApJ, 677, 169
Villar V., Gallego J., Pérez-Gonzàlez P. G., Barro G., Zamorano J., Noeske K., Koo D. C., 2011, ApJ, 740, 47
Vučetić M. M., Arbutina B., Urošević D., Dobardžić A., Pavlović M. Z., Pannuti T. G., Petrov N., 2013, Serbian Astron. J., 187, 11
Vukotić B., Bojičić I., Pannuti T. G., Urošević D., 2005, Serbian Astron. J., 170, 101
Walter F., Weiss A., Martin C., Scoville N., 2002, AJ, 123, 225
Williams R. M., Chu Y.-H., Dickel J. R., Petre R., Smith R. C., Tavarez M., 1999, ApJS, 123, 467
Williams B. F., Sjouwerman L. O., Kong A. K. H., Gelfand J. D., Garcia M. R., Murray S. S., 2004, ApJ, 615, 720
Yang H., Skillman E. D., Sramek R. A., 1994, AJ, 107, 651
Ye T., 1988, PhD thesis, Univ. Sidney
Ye T., Turtle A. J., Kennicutt R. C., 1991, MNRAS, 249, 722

APPENDIX A: OPTICAL SNRS IN NEARBY GALAXIES

This is a sample of Table A1. The complete Table A1, as well as Tables A2 to A18, are available in the Online Appendix and at http://poincare.matf.bg.ac.rs/~arbo/catalogue/ .

Table A1. Optical SNRs in the M31 galaxy.[a]

Object name	RA (J2000.0) (h)	Dec. (J2000.0) (°)	F(H α) (erg cm^{-2} s^{-1}) $\times 10^{-15}$	Diameter (arcsec)	[S II]/H α ratio
1	9.4056797	39.862778	7.8	12.9	0.86
2	9.8472862	40.738834	51.5	15.3	1.06
3	9.8783941	40.357998	7.1	8.8	0.96
4	9.9373655	40.498367	31.8	12.6	1.09
5	9.9593277	40.349838	43.9	14.8	0.40
6	9.968482	40.495148	112.7	19.6	0.67
...	...	...	...	...	...
156	11.6789007	42.21674	9.2	13.6	1.12

[a]Data taken from Lee & Lee (2014).

SUPPORTING INFORMATION

Additional Supporting Information may be found in the online version of this article:

(http://mnras.oxfordjournals.org/lookup/suppl/doi:10.1093/mnras/stu2093/-/DC1).

Please note: Oxford University Press are not responsible for the content or functionality of any supporting materials supplied by the authors. Any queries (other than missing material) should be directed to the corresponding author for the article.

This paper has been typeset from a TEX/LATEX file prepared by the author.